ACS OMEGA

Open Access

http://pubs.acs.org/journal/acsodf

Article

Comparative Study of the Structure and Height of CH_4 Laminar Diffusion Flames: Effects of Fuel-Side versus Air-Side Dilution

Huanhuan Xu, Guangdong Zhou, Zilin Zhu, and Zhiqiang Wang*

Cite This: *ACS Omega* 2024, 9, 1113−1124

Read Online

ACCESS | Metrics & More | Article Recommendations

ABSTRACT: The strategy for introducing diluents is a critical practical concern in diluted combustion; however, a comprehensive understanding of the effects of fuel-side dilution versus air-side dilution is currently lacking. This numerical investigation systematically studied the effects of dilution strategies on methane coflow diffusion flames, with a focus on the flame structure and flame length. Common additives in practical combustion, specifically H_2O and CO_2, were introduced to either the fuel or the air streams, with dilution ratios (Z) ranging from 0 to 0.2, and the impacts of four dilution strategies were quantified and ranked. Detailed simulations were conducted using a well-validated two-dimensional (2D) flame code to gain a deep understanding of OH formation, flame attachment, temperature of the burner nozzle, and flame height. Systematic analyses in terms of heat transfer, molecular diffusion, and chemical kinetics were conducted. Results demonstrate that introducing diluents into the air stream exerts a more profound influence on suppressing OH formation compared with fuel-side dilution. Moreover, air-side dilution has a negligible influence on flame attachment, while increasing Z on fuel side significantly inhibits flame attachment, and the latter behavior is attributed to the diminished mass diffusion of CH_4 toward the oxidizer side. As the flame attachment weakens, it causes a consequential reduction in heat transfer from the flame base to the burner. Accordingly, the nozzle temperature exhibits a more remarkable decrease with the fuel-side dilution ratio than with the air-side dilution ratio. Simultaneously, a more profound influence of Z on flame length was observed for fuel-side dilution than for air-side dilution, and the underlying mechanisms governing these two distinct dilution strategies were theoretically elucidated.

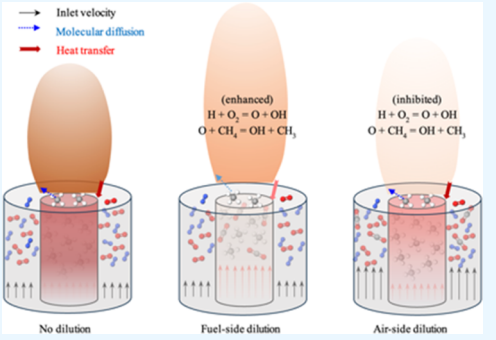

1. INTRODUCTION

Diluted combustion stands as a widely employed strategy in various industrial applications due to its efficacy in lowering flame temperatures and curbing pollutant emissions. This approach encompasses technologies like flue gas recirculation and oxy-fuel combustion,[1−4] among others. Notably, in the pursuit of a carbon-neutral future, advanced combustion methodologies such as steam dilution combustion and oxy-fuel combustion have emerged as highly promising. These technologies involve the enrichment of CO_2 within the flue gas, facilitating cost-effective CO_2 capture.[5−7]

To gain a comprehensive understanding of the impact of dilution on the combustion process, existing research has predominantly focused on two key factors: the type of diluent and the level of dilution. The choice of diluent introduces inconsistent alterations to the combustion process due to variations in their thermal, chemical, and diffusion parameters, while the dilution ratio modulates the extent of their influence. However, the exploration of the dilution strategy, specifically the position at which diluents are introduced (on either the fuel side or the air side), has been relatively scarce. This investigation is indispensable, particularly when considering practical applications, as the dilution position significantly influences the flow dynamics and the mixing process in the early stage of combustion.

Though limited in number, studies comparing air- and fuel-side dilutions for jet diffusion flames have been reported. Cho and Chung[8] experimentally examined the effects of flue gas dilution on NOx emissions using a swirl diffusion burner. Their findings indicated that NO reduction is more pronounced when N_2 dilution occurs on the fuel side as opposed to the oxidizer side. Feese and Turns[9] conducted experimental investigations to assess the impact of N_2 dilution on laminar CH_4 jet diffusion flames, and they found that air-side dilution is more effective in reducing NOx emissions compared to fuel-side dilution. Additionally, they noted that the visible flame height slightly increases with the addition of diluent into the air flow but remains relatively stable for fuel-side dilution. Lock et

Received: September 25, 2023
Revised: November 1, 2023
Accepted: December 5, 2023
Published: December 19, 2023

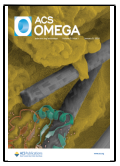

https://doi.org/10.1021/acsomega.3c07406
ACS Omega 2024, 9, 1113−1124

al.[10] explored the efficacy of dilution in the fuel stream versus the air stream to extinguish laminar methane-air partially premixed and diffusion flames using CO_2, and found that as the level of premixing increased, fuel-side dilution becomes more effective in extinguishing the flame compared to air-side dilution. Marin and Baillot[11] conducted experimental research with a focus on the leading edge of an attached non-premixed methane-air flame. They compared the effects of air-side versus fuel-side dilution with a particular emphasis on flame lifting characteristics.

Obviously, existing investigations on dilution strategies were mainly focused on general combustion properties, such as flame stability, NOx emissions, and flame height, while providing limited insights into the intricate physical processes and chemical kinetics. A comprehensive understanding of essential flame characteristics, including structure and tightly related combustion kinetics, remains notably underdeveloped for practical jet flames, which are usually multidimensional.

Nevertheless, in addressing the impact of the diluent type and dilution ratio, there exists a substantial body of relevant literature. To provide a thorough overview of the state of the art, a brief review of the literature pertaining to both general combustion behavior and combustion kinetics is undertaken here.

First, in pursuit of practical applications, experimental investigations were conducted on diluted combustion in jet flames. Erete et al.[12] examined the impact of CO_2 dilution on the fuel side on turbulent non-premixed methane-air jet flames. They observed that CO_2 dilution reduces flame height and raises the flame attachment point while also decreasing NOx emissions by lowering peak temperatures. Liu et al.[13] experimentally explored the effects of CO_2, N_2, and CO_2/N_2 dilution on the combustion characteristics of a turbulent, partially premixed CO/H_2-air flame. Their results revealed that CO_2- and CO_2/N_2-diluted flames have larger reaction zones compared to N_2-diluted flames. Vadel et al.[14] investigated the influence of adding H_2O and CO_2 to the fuel flow in swirled methane/oxygen-enriched air flames. Their findings indicated that CO_2 dilution increases the flame height and the flame-lift height to a larger extent than H_2O dilution.

Second, to gain fundamental insights into the impact of diluent addition on combustion kinetics, a burner configuration with a simple geometry is commonly employed, such as counterflow diffusion flames. These flames can be simplified as one-dimensional, which benefits computational efficiency. Liu et al.[15] studied the chemical effects of CO_2 added to either the fuel side or the oxidizer side on ethylene counterflow diffusion flames. They identified that the reaction $CO_2 + H = CO + OH$ plays a pivotal role in soot and NOx formation. Wang et al.[16] conducted similar investigations, noting that CO_2 addition to the oxidizer flow increases CO production through $CO_2 + H = CO + OH$, and the promoted forward progress of this elemental reaction reduces H concentration, which accordingly further increases CO production through $HCO = H + CO$. Additionally, Watanabe and Glaborg et al.[17,18] discovered that CO_2 dilution on the fuel side increases the mole fraction of OH and CO when methane burned under oxy-fuel conditions, as a result of the promoted forward progress of the reaction $CO_2 + H = CO + OH$. While these studies based on 1D flames greatly contribute to understanding diluted combustion in detail, they do not provide direct guidelines for practical combustor applications.

There accordingly arises a question: Is there a flame configuration that can faithfully replicate the multidimensional combustion behaviors observed in real combustors while remaining suitable for flame modeling, enabling a deep understanding of the detailed combustion kinetics? Laminar coflow diffusion flames appear to offer a compelling solution. Notably, they encompass multidimensional aspects encompassing flow dynamics, heat transfer, diffusion, and chemical reactions, making them an indispensable multidimensional flame model for comprehending the intricate physical and chemical processes within practical combustion devices. Furthermore, unlike counterflow diffusion flames, laminar coflow diffusion flames provide a more comprehensive data set which is vital for the development and operation of combustors. This data set includes critical factors such as combustion intensity, flame stability, flame size, and more.

Actually, many researchers have studied the diluted laminar coflow flames to compare the effect of either the diluent type or dilution ratio, but again, an understanding of the difference in dilution position is still missing. Min et al.[19] studied the impact of CO_2-, N_2-, and Ar-diluted air on the flame length and lifting behavior of a laminar diffusion flame, and they found that when keeping the air flow rate constant, all of these diluents increase flame height. Tu et al.[20] experimentally and numerically examined the effects of different diluents (N_2, CO_2, and H_2O) on the flame characteristics of CH_4/H_2-blended fuel in a jet-in-hot-coflow burner, and they concluded that the chemical effects of CO_2 and H_2O result in the ignition delay, and the ignition delay distance is further enlarged for H_2O-diluted cases when compared with CO_2-diluted cases. Xu et al.[21] investigated the effects of H_2O- and CO_2-diluted oxidizers on the structure and shape of laminar coflow syngas diffusion flames, and they pointed out that the higher concentrations of OH under H_2O addition lead to the decreased flame height, while the addition of CO_2 suppresses flame temperature and results in increased flame height. Cepeda et al.[22] experimentally and numerically studied the influence of water vapor in oxidizer stream on laminar coflow ethylene diffusion flames. They found that H_2O addition affects the concentrations of H and OH and accordingly alters the formation and oxidation of the soot precursors. To sum up, the laminar coflow flame provides such a combustion model to simultaneously study detailed combustion processes and general combustion performances.

The present study is a follow-up to our previous work, ref23, where we investigated the influence of fuel-side versus oxidizer-side dilutions on NO emissions in CH_4 counterflow diffusion flames. Expanding on this basis, the objectives of this study are 2-fold: (1) to compare the effects of fuel-side versus oxidizer-side dilution on the general characteristics of a more application-relevant multidimensional flame and (2) to illustrate how dilution strategy alters the detailed flame structure and general flame height of a laminar coflow CH_4 diffusion flame from the perspectives of heat transfer, molecular diffusion, and chemical kinetics.

In this numerical study, CO_2 and H_2O, as common diluents, were chosen to be investigated. A dilution parameter Z was defined to ensure that the flame characteristics were comparable between dilutions occurring at the fuel side and air side. Z ranged from 0 to 0.2, and all of the investigations were conducted at 1 atm and 400 K. Based on the detailed simulations, the effects of fuel-side dilution versus air-side dilution were comprehensively studied, and this article is

https://doi.org/10.1021/acsomega.3c07406
ACS Omega 2024, 9, 1113−1124

structured as follows: The influence of different dilution strategies on OH formation was first investigated to exhibit an overall flame structure; then, more detailed flame structure of the flame base was studied by analyzing the flame attachment and how it affects the burner nozzle temperature, and illustrations on levels of molecular diffusion and combustion kinetics were made; and, finally, the flame height was investigated and theorical analyses were performed.

2. EXPERIMENTAL AND SIMULATION METHODS

A two-dimensional (2D) Fortran flame simulation program was used to study the diluted laminar coflow diffusion CH_4 flames in this work. More information about this flame code can be found in Liu et al.[24,25] This Fortran flame code couples almost all of the chemical and physical submodels related to the flow, heat transfer, diffusion, and chemical reactions in the combustion process. The SIMPLE algorithm was adopted to deal with the coupling problem of pressure and velocity. CHEMKIN program package was incorporated to calculate the thermodynamic and transport parameters of the chemical reactions, by which the detailed simulation of the combustion process could be achieved. The detailed chemical mechanism GRI 3.0 was used in this work. Since NOx emission is not the emphasis in this study, all of the chemical reactions relating to NOx formation were excluded, which led to 36 species and 219 elementary reactions left. The negligible effect of excluding the relevant NOx reactions has been evaluated previously. Discrete-ordinates method (DOM) was used to solve the process of radiation transfer, and the absorption coefficients of CO_2 and H_2O were calculated based on the statistical narrow-band correlated-K radiation model (SNBCK).[26] The SORET effect[27] was considered to precisely calculate the preferential diffusion of light components such as H and H_2. The governing equations, including continuity equation, axial momentum equation, radial momentum equation, energy equation, and composition equation, were discretized using the finite volume method. In addition, soot formation was modeled using a semiempirical two-equation model,[24] in which acetylene is the only species responsible for soot nucleation and surface growth.

The computational domain is shown in Figure 1. The fuel stream was injected through the center tube, and the air comes out from the coaxial oxidizer tube. The inner diameters of the fuel tube and the oxidizer tube were 3.06 and 25.4 mm, respectively. Detailed dimensions are defined in Xu et al.[28] This study set the inlet boundary below the nozzle tip, which means that a certain length of the burner wall was also modeled in the computational domain. The left axis was an asymmetric boundary, the exit boundary of the upper calculation region was set as the zero-gradient condition, and the right edge of the computational domain was free slip.

Since the cross-sectional area of the fuel tube is much smaller than that of the oxidizer tube, introducing the same amount of the diluent into the fuel tube and the air tube causes a great difference in velocity variations. To ensure that the flame characteristics for fuel-side and oxidizer-side dilutions are comparable, a dilution parameter Z was introduced in this work, defined as the ratio of the mass of the diluent to the mass of the stoichiometric mixture. As this parameter is calculated based on the mass of the stoichiometric mixture instead of the fresh fuel or air flow, the influence of the dimension difference of the fuel/air tubes on the dilution level was eliminated. This

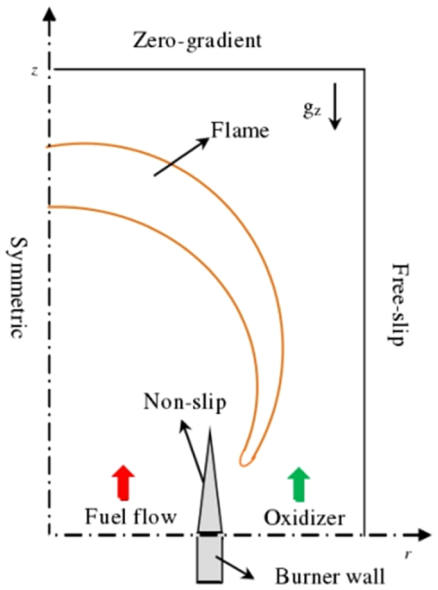

Figure 1. Boundaries of the coflow diffusion flame simulation.

parameter was proposed by Feese and Turns[9] for diluted diffusion flames, as shown in eq 1.

$$Z = f_s \frac{Y_{dil,F}}{1 - Y_{dil,F}} + (1 - f_s)\frac{Y_{dil,A}}{1 - Y_{dil,A}} \quad (1)$$

where $Y_{dil,F}$ and $Y_{dil,A}$ represent the mass fractions of the diluent in fuel-side dilution and air-side dilution, respectively, and f_s is the stoichiometric mixture fraction.

For a given dilution parameter, the dilution levels near the flame front were the same. A wide range of Z values was investigated in this study, varying from 0 to 0.20. With the dilution parameter Z, the flow rates of fuel and air streams were then calculated: conditions for the CO_2 and H_2O dilutions are shown in Tables 1 and 2, respectively. The flow rate of

Table 1. Conditions for the CO_2 Dilution (1 atm, 400 K)

		fuel side (L/min)		air side (L/min)		
case no.	Z	CH_4	CO_2	O_2	CO_2	N_2
0	0	0.05	0	1.05	0	3.95
C_1	0.05	0.05	0.0166	1.05	0	3.95
C_2	0.1	0.05	0.0332	1.05	0	3.95
C_3	0.15	0.05	0.0498	1.05	0	3.95
C_4	0.2	0.05	0.0664	1.05	0	3.95
C_5	0.05	0.05	0	1.05	0.1734	3.95
C_6	0.1	0.05	0	1.05	0.3467	3.95
C_7	0.15	0.05	0	1.05	0.5201	3.95
C_8	0.2	0.05	0	1.05	0.6935	3.95

methane was fixed at 0.05 L/min, and the flow rate of air was consistently set as 5 L/min (with the flow rate of oxygen being 1.05 L/min, CH_4 could be completely burned). The largest Re in this work was less than 310, so all of the flames simulated here were in a laminar regime. The Froude number (Fr) ($U_{fuel}^2/(gd)$, where U_{fuel} is the outlet velocity of the fuel stream, g is the gravitational acceleration, and d is diameter of the fuel tube, i.e., 3.06 mm) varied from 2.93 to 15.85. It can be seen that C_3−C_4 and H_2−H_4 were momentum driven, and the rest of the investigated flames were buoyancy driven. Based on the

https://doi.org/10.1021/acsomega.3c07406
ACS Omega 2024, 9, 1113−1124

Table 2. Conditions for the H_2O Dilution (1 atm, 400 K)

		fuel side (L/min)		air side (L/min)		
case no.	Z	CH_4	H_2O	O_2	H_2O	N_2
0	0	0.05	0	1.05	0	3.95
H_1	0.05	0.05	0.0406	1.05	0	3.95
H_2	0.1	0.05	0.0811	1.05	0	3.95
H_3	0.15	0.05	0.1217	1.05	0	3.95
H_4	0.2	0.05	0.1622	1.05	0	3.95
H_5	0.05	0.05	0	1.05	0.4238	3.95
H_6	0.1	0.05	0	1.05	0.8476	3.95
H_7	0.15	0.05	0	1.05	1.2713	3.95
H_8	0.2	0.05	0	1.05	1.6951	3.95

flow rates given in Tables 1 and 2, the velocities of the fuel and oxidizer streams at the burner exit plane are shown in Table 3.

Table 3. Gas Flow Velocities for CO_2 and H_2O Dilutions

		CO_2 dilution		H_2O dilution	
	Z	U_{fuel} (cm/s)	U_{air} (cm/s)	U_{fuel} (cm/s)	U_{air} (cm/s)
no dilution	0	29.63	24.97	29.63	24.97
fuel-side dilution	0.05	39.46	24.97	53.66	24.97
	0.1	49.29	24.97	77.68	24.97
	0.15	59.12	24.97	101.71	24.97
	0.2	68.95	24.97	125.74	24.97
air-side dilution	0.05	29.63	25.84	29.63	27.09
	0.1	29.63	26.7	29.63	29.2
	0.15	29.63	27.57	29.63	31.32
	0.2	29.63	28.43	29.63	33.44

3. RESULTS AND DISCUSSION

3.1. Validation of the Flame Model. It is worth pointing out that the case $Z = 0$ is identical to that of the CH_4/air diffusion flame in the previous work of Xu et al.,[28] where measurements were performed. Despite the fact that the accuracy of the simulation method in this study is already validated in that work, experimental and numerical results are still exhibited here for a quick visual comparison. According to the flame spectrum, the yellow flame tip of hydrocarbon fuels is caused by the continuous radiation of the high-temperature soot particles in the visible-light wavelength, which is common knowledge regarding soot formation, as mentioned by Li et al.[29] It can be seen that the visible flame height (flame yellow part) in Figure 2a is about 9 mm, while the computed flame height (top of the soot area) is about 9.6 mm, which is close to the experiment. Therefore, the numerical results analyzed in this work can be considered as accurate.

3.2. OH Formation. Figure 3a−e shows the distributions of OH mole fraction of CH_4 flames with or without CO_2 dilution. It is clear that the increasing dilution parameter Z decreases OH concentration, which is consistent with the findings of Xu et al. that CO_2 addition suppresses OH concentration when they replace N_2 in the air with CO_2.[21] The effects of CO_2 dilution on decreasing OH mole fraction correlate well with the trend of the flame temperature. Simulation data show that the flame temperature peak is 2070.5 K for the undiluted flame ($Z = 0$) and 1940.1 and 1937.5 K for fuel-side and air-side CO_2 dilutions at $Z = 0.15$, respectively. Both the inhibited OH formation and lowered temperature imply the weakened combustion intensity, which agrees with the conclusion of Wang et al.[16]

In addition, a very interesting and novel phenomenon observed in Figures 3 and 4 is that air-side dilution has a greater influence on decreasing OH formation than fuel-side dilution, consistent with both H_2O and CO_2 dilutions. For example, in Figure 3a,b, the OH maximum mole fraction of the fuel-side-diluted flame reduced from 6.17×10^{-3} at $Z = 0$ to 5.63×10^{-3} at $Z = 0.05$ in Figure 3d, while this fraction reaches a smaller value of 5.45×10^{-3} when dilution occurs in air side with the same Z. In Figure 4b,d, when $Z = 0.05$, the OH maximum mole fractions are 5.79×10^{-3} and 5.36×10^{-3} for fuel-side and air-side dilutions, respectively. Constantly, the impact is more profound for air-side dilution than fuel-side dilution. When Z increases to 0.15, the suppressing influence of CO_2 or H_2O dilution on OH formation has a similar trend but with a greater degree than that of $Z = 0.05$.

There are two main factors affecting the OH concentration in Figures 3a−e and 4a−e.

The first is the dilution effect. The dilution effect changes the combustion process by lowering the concentration of reactant components.[25] Specifically, depending on whether it is added into the fuel flow or the air flow, the amount of the added diluent increases differently, as shown in Tables 1 and 2. Given the same Z, the flow rate of diluents (both CO_2 and H_2O) injected into the fuel stream is less than that into the air stream. For example, the flow rate of CO_2 for fuel-side dilution is 0.0166 L/min while it is 0.1734 L/min for air-side dilution at

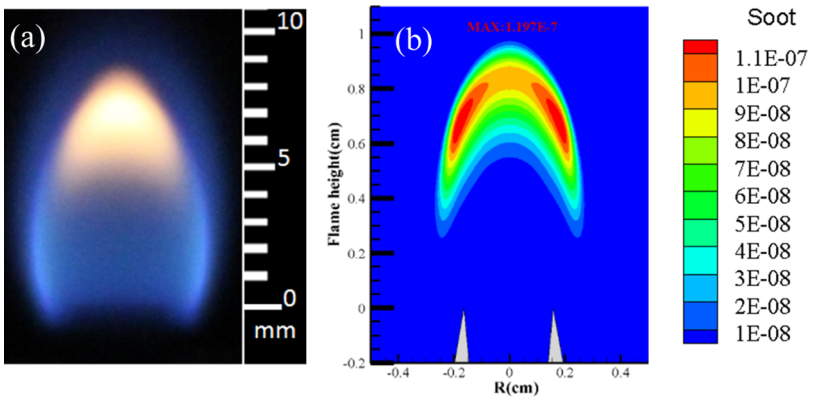

Figure 2. Flame photograph (a, reproduced with permission from ref 28. Copyright 2018, Elsevier) and the computed soot volume fraction (b) of undiluted CH_4/air coflow laminar diffusion flames ($Z = 0$). The gray shade in (b) indicates the fuel tube nozzle.

https://doi.org/10.1021/acsomega.3c07406
ACS Omega 2024, 9, 1113−1124

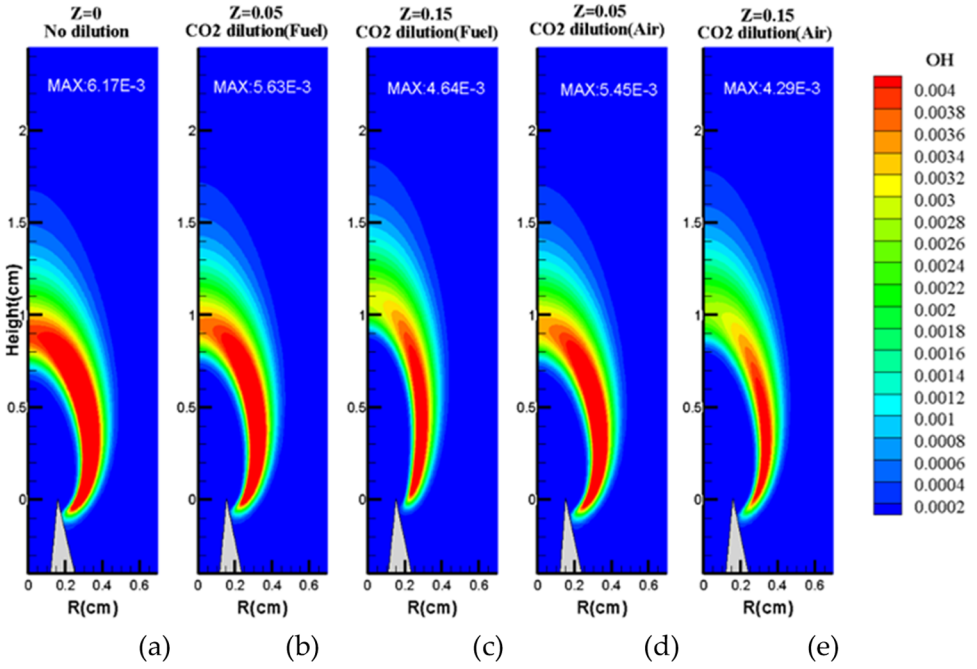

Figure 3. Computed OH mole distributions under various CO_2 fuel-side and air-side dilution levels.

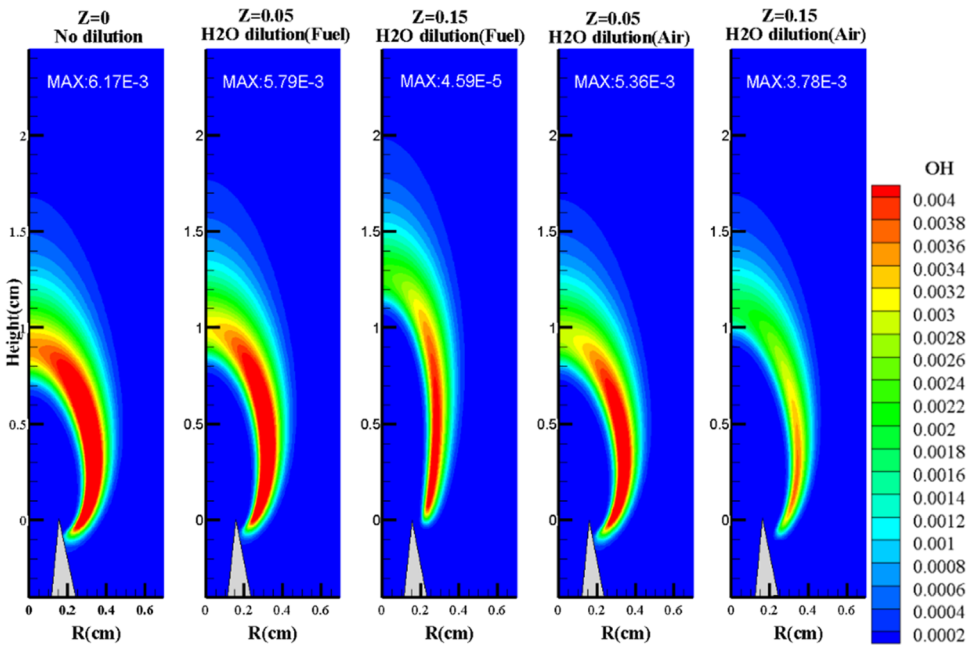

Figure 4. Computed OH mole distributions under various H_2O fuel-side and air-side dilution levels.

Z = 0.05; as a result, air-side dilution lowers the OH concentration with a greater degree than fuel-side dilution through the dilution effect. Besides, for the same Z, the amount of added H_2O is much larger than that of CO_2, as shown in Tables 1 and 2; thus, H_2O dilution generally has a greater effect on decreasing OH formation than that of CO_2, as shown in Figures 3a−e and 4a−e.

The second is the chemical effect, namely, diluents taking part in the reactions during combustion. OH production rates at HAB (Height above burner) = 0 mm are shown in Figures 5 and 6. Figure 5 shows OH production rates of the main reactions for CO_2 dilution at Z = 0 and Z = 0.05. It can be observed in Figure 5 that CO_2 dilution in the fuel side promotes the reaction of R38 which increases the OH formation and promotes reactions involving R97, R98, R99 and R101, and as a result, OH consumption is enhanced. Overall, the suppressing effects of CO_2 dilution on OH formation overwhelm its enhancing impact, and the chemical effect of CO_2 dilution in fuel side inhibits OH formation. When dilutions occur in the fuel side, OH production and consumption are affected similarly to the air-side dilution except for dilutions in R38 and R11. A summary of some essential elementary reactions is given in Table 4. Air-side dilution inhibits the forward process of reactions R38 and R11, but fuel-side dilution promotes them, especially R38. Since the forward process of R38 and R11 leads to OH formation, this

https://doi.org/10.1021/acsomega.3c07406
ACS Omega 2024, 9, 1113−1124

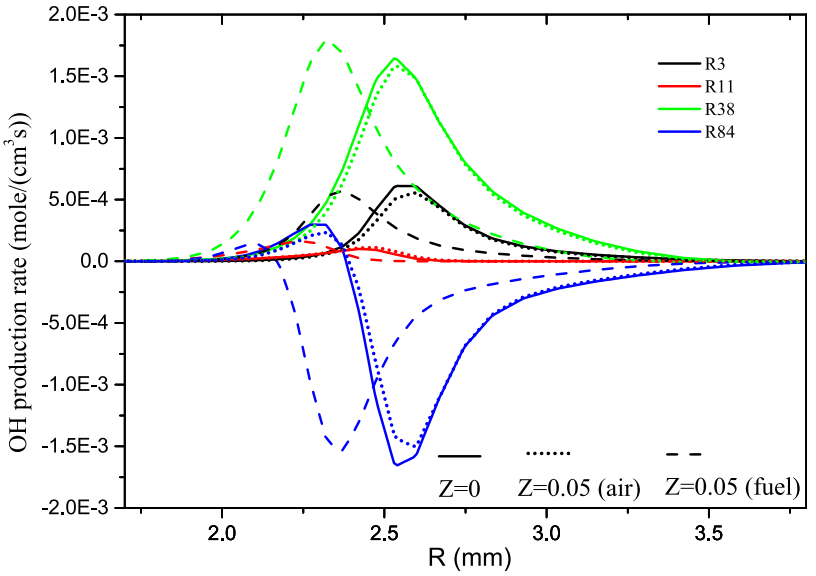

Figure 5. OH production rates of main reactions at HAB = 0 mm with CO_2 dilution in the fuel side and air side when Z = 0 and Z = 0.05.

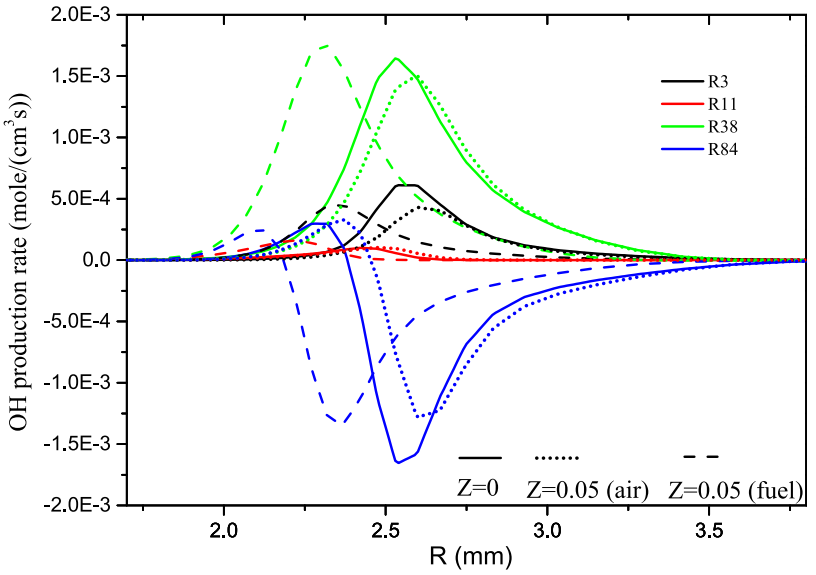

Figure 6. OH production rates of main reactions at HAB = 0 with H_2O dilution in the fuel side and air side when Z = 0 and Z = 0.05.

Table 4. Summary of Some Important Elementary Reactions Related to OH Formation

reaction no.	reaction steps
R3	$O + H_2 = H + OH$
R11	$O + CH_4 = OH + CH_3$
R38	$H + O_2 = O + OH$
R84	$OH + H_2 = H + H_2O$
R97	$OH + CH_3 = CH_2(S) + H_2O$
R98	$OH + CH_4 = CH_3 + H_2O$
R99	$OH + CO = H + CO_2$
R101	$OH + CH_2O = HCO + H_2O$

kinetics difference explains the greater influence of air-side dilution on OH formation than fuel-side dilution.

Compared with Figures 5 and 6 shows a similar phenomenon of OH production rates of main reactions for H_2O dilution at Z = 0 and Z = 0.05, but there are still some differences. For example, H_2O dilution inhibits R3 and R84 (more noticeable) in both sides' dilution and inhibits R38 in air-side dilution; besides, it promotes R98 in both sides' dilution. When a small amount of H_2O is added, like fuel-side dilution at Z = 0.05, its chemical effect may enhance OH formation, as reported in ref 25, and this might explain why maximum OH mole fraction in Figure 4b is higher than that in Figure 3b.

3.3. Flame Attachment. The structure of the flame base provides crucial information about combustion initiation and plays a significant role in governing flame stability. Since it is dominated by the flow time scale and the chemical time scale, adding diluents could change the flame base through modifications in any of these aspects. Flame base is of particular importance for two safety concerns: on the one hand, when the flame base anchors to the fuel tube nozzle, i.e., flame attachment occurs, the remarkable preheating effect protects the flame brush from blowout, and the flame stability

https://doi.org/10.1021/acsomega.3c07406
ACS Omega 2024, 9, 1113−1124

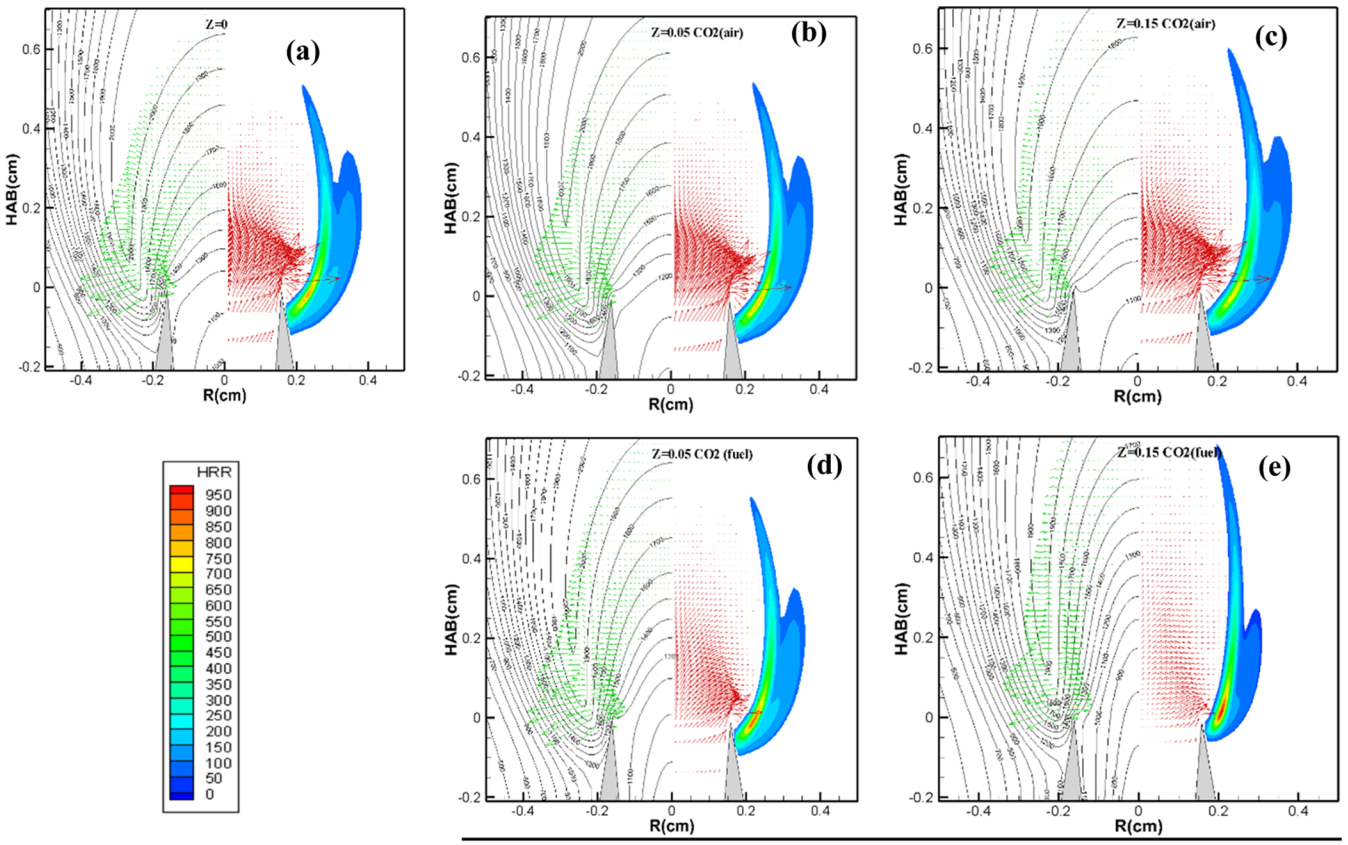

Z	0	0.05(fuel)	0.15(fuel)	0.05(air)	0.15(air)
CH_4	9.38E-06	4.53E-06	1.87E-06	9.47E-06	9.50E-06
CH_3	1.20E-11	1.15E-11	9.95E-12	1.09E-11	8.54E-12
Maximum *HRR*	800	852	939	772	711
Temperature (K)	2072.20	2036.10	1943.10	2025.00	1939.20
DFA (cm)	-0.12	-0.10	-0.06	-0.12	-0.12

Figure 7. Computed diffusion mass flux vectors of CH_4, CH_3 (g/(cm^2·s)), heat release rate (J/(cm^3·s)), temperature (K), and flame attachment depth without dilutions (a), and with CO_2 dilution in air side (b, c) and fuel side (d, e).

is enhanced; on the other hand, a severe flame attachment might cause massive heat transfer to the tube, and material damage might happen to the burner nozzle due to the terribly high temperature, and this point is discussed in Section 3.4.

The addition of diluents into either the fuel flow or the air flow increases the outlet velocity, as shown in Table 3, but with different effects on the flame attachment. Figure 7 shows detailed structures of the flame base for Cases 0 and C_1−C_8, including the computed diffusion mass flux vectors of CH_4 and CH_3 and the heat release rates (HRRs). The depths of the flame attachment (DFAs) were identified as the lowest axial position of a value of 10% of the maximum heat release rate, as used in the study of Xu et al.,[28] which are also marked in Figure 7. It is apparent that addition of CO_2 into the fuel tube reduces DFA; specifically, DFAs decrease with increasing the dilution parameter from −0.12 mm at Z = 0 to −0.06 mm at Z = 0.05. In contrast, air-side dilution exerts almost no influence on flame attachment, as DFA remains approximately at −0.12 mm for all of the cases with Z less than 0.15. Particularly, the negative sign indicates that the flame attachment point is below the burner exit.

To understand the difference between the effects of air-side and fuel-side dilutions on the flame attachment, the fuel jet velocity and the mass diffusion flux of methane are discussed next.

When the jet velocity of the fuel flow is small, the residence time is considerably sufficient compared with the chemical reaction time; consequently, combustion occurs immediately once the mixture reaches a nearly stoichiometric ratio. On the one hand, as more diluents were added into the fuel tube, and the velocity of the oxidizer flow remains constant (Case 0 to Cases C_1−C_4), the relative velocity of the fuel flow to the oxidizer flow increases (U_{fuel}/U_{air} increases from 1.18 at Z = 0 to 2.76 at Z = 0.2) and more fuel reaches the oxidizer side convectively. On the other hand, as more CO_2 is added into the fuel tube, CH_4 concentration in the fuel stream is reduced, subduing the mass diffusion of the fuel into the oxidizer flow, as shown in Figure 7. CH_4 mass flux vectors of the fuel-side-diluted flame reduced from 9.38×10^{-6} g/(cm^2·s) at Z = 0 to 4.53×10^{-6} g/(cm^2·s) at Z = 0.05, while these vectors reach a smaller value of 1.87×10^{-6} g/(cm^2·s) at Z = 0.15. The penetration of the fuel toward the outside of the burner is enhanced through the convection process, and apparently, this increased value does not overwhelm that suppressed value by mass diffusion. As a result, the stoichiometric mixture appears at a more downstream position outside the nozzle, and the flame attachment is inhibited.

https://doi.org/10.1021/acsomega.3c07406
ACS Omega 2024, 9, 1113−1124

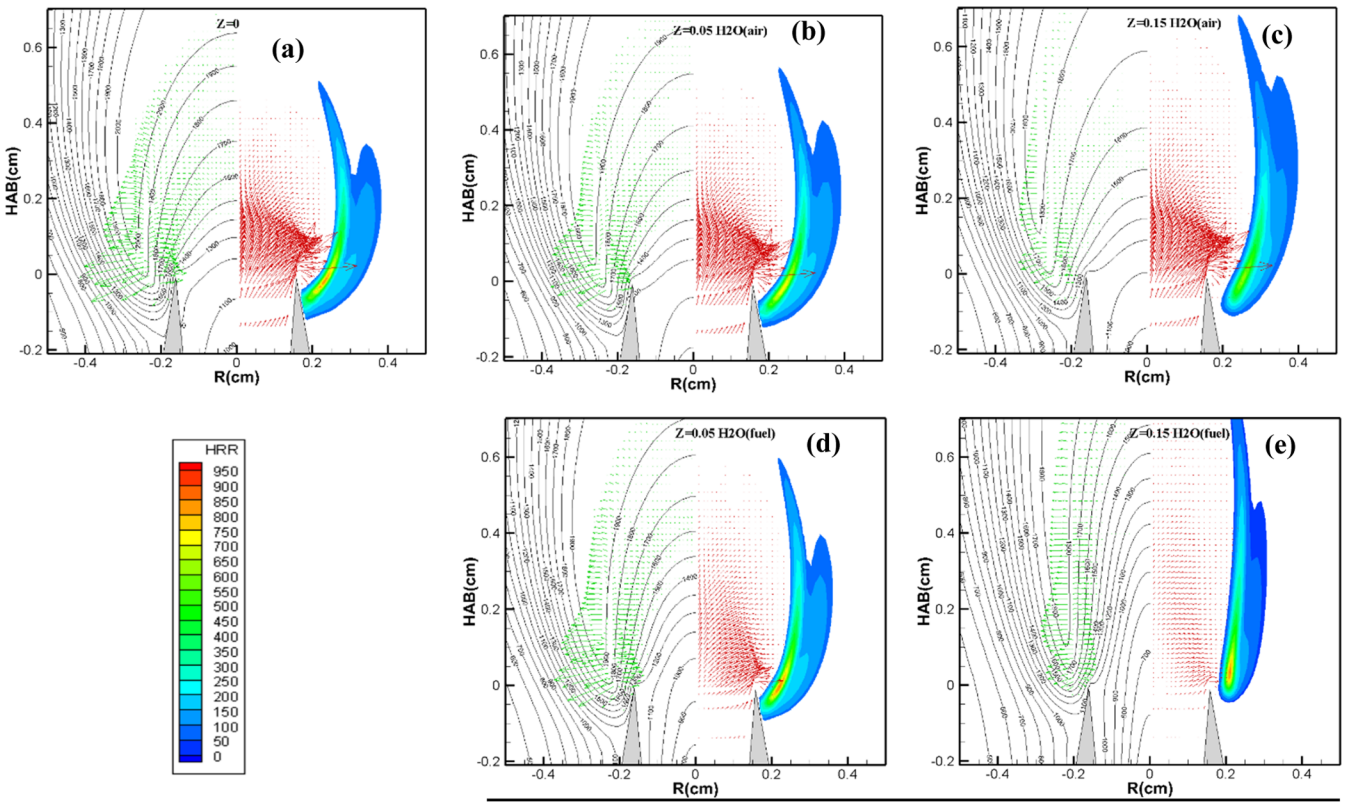

Z	0	0.05(fuel)	0.15(fuel)	0.05(air)	0.15(air)
CH_4	9.38E-06	3.47E-06	9.97E-07	9.45E-06	9.60E-06
CH_3	1.20E-11	9.96E-12	6.39E-12	9.14E-12	5.12E-12
Maximum *HRR*	800	816	816	703	591
Temperature (K)	2072.20	2014.20	1880.90	1979.80	1835.60
DFA (cm)	-0.12	-0.09	-0.04	-0.12	-0.11

Figure 8. Computed diffusion mass flux vectors of CH_4, CH_3 (g/(cm^2·s)), heat release rate (J/(cm^3·s)), temperature (K), and flame attachment depth without dilutions (a), and with H_2O dilution in air side (b, c) and fuel side (d, e).

As more diluents were added into the air stream by keeping the velocity of fuel flow constant (Cases 0 to C5−C8), the relative velocity of the fuel flow to the oxidizer flow slightly decreased (U_{fuel}/U_{air} decreases from 1.18 at Z = 0 to 1.04 at Z = 0.2), and the amount of fuel that reaches the oxidizer side through the convection process is almost unchanged. In Figure 7, it is also observed that the mass diffusion flux of CH_4 remains constant when flames are diluted in the air side. CH_4 mass flux vectors of the fuel-side-diluted flame increased from 9.38×10^{-6} g/(cm^2·s) at Z = 0 to 9.47×10^{-6} g/(cm^2·s) at Z = 0.05, and these vectors reached a slightly larger value of 9.50×10^{-6} g/(cm^2·s) at Z = 0.15. Thus, the stable convection combined with the diffusion of CH_4 from the fuel tube to the outside of the burner determines the negligible influence of air-side dilution on the flame attachment.

To understand the flame attachment for cases of H_2O dilution, Figure 8 shows a comparison of the combustion information near the flame base at Z = 0, Z = 0.05, and Z = 0.15. DFAs are −0.12 mm, −0.09 mm, and −0.04 mm when H_2O dilutes fuel side at Z = 0, Z = 0.05, and Z = 0.15, respectively, while they are −0.12 mm, −0.12 mm, and −0.11 mm, when H_2O dilutes air side at Z = 0, Z = 0.05, and Z = 0.15, respectively. The effects of air-side and fuel-side H_2O dilutions on flame attachment are very similar to those of CO_2 dilutions.

In conclusion, both CO_2 and H_2O dilutions in the fuel-side lift the flame base because of the reduced diffusion mass flux of CH_4 as a result of the lower CH_4 fraction in the fuel flow. In addition, the relative velocity of the fuel flow to the oxidizer flow also changes but alters only the flame attachment with very little contribution.

3.4. Temperature of the Burner Nozzle. When the flame attaches to or gets close to the burner nozzle, a high temperature could shorten the service life of nozzles, and the temperature of the burner nozzle is a critical parameter to take precautions. In this section, we discuss and analyze the temperature of the burner nozzle (TBN) under different dilution strategies. For the sake of clarity, the computed TBN is defined as the temperature of the nozzle tip, namely, at the location r = 1.5 mm and HAB (height above the burner) = 0 mm.

Figure 9 compares the effects of fuel-side and air-side dilutions on the temperature of the burner tip, and black plots represent CO_2 dilutions while blue plots are H_2O dilutions. It is clear that TBNs decrease with more diluent addition, and a more profound impact can be observed for fuel-side dilutions. For example, for CO_2 dilution at Z = 0.05, the nozzle temperature is 1181 K for fuel-side dilution and 1208 K for air-side dilution; at a larger Z of 0.20, the nozzle temperatures

https://doi.org/10.1021/acsomega.3c07406
ACS Omega 2024, 9, 1113−1124

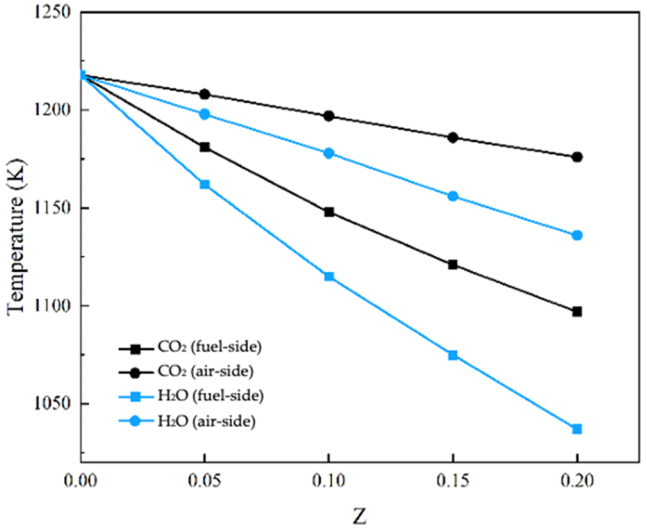

Figure 9. Computed nozzle tip temperature with CO_2 and H_2O dilutions in fuel side vs air side.

become lower and are 1097 and 1176 K when dilution occurs in fuel side and air side, respectively.

Generally speaking, there are three aspects affecting TBN: (1) the thermal level at the flame base, i.e., HRR; (2) the thermal resistance between the flame and the burner nozzle, mainly depending on the distance between the flame front and the nozzle; and (3) the cooling capacity of the fluid near the nozzle. Since the fuel tube was always enveloped by the flame base under all of the investigated conditions, no fresh oxidizer flow contacted the burner tip directly, leading to the cooling capacity dominated by the velocity of the fuel flow. Besides, the fuel-side dilution increases U_{fuel} to a much larger extent than that air-side dilution increases U_{air}, as shown in Table 3, which further emphasizes the importance of the convective heat transfer.

First, the heat release rate increases with increasing CO_2 dilution for fuel-side dilutions as Figure 7 shows that the maximum HRR is enhanced from 800 J/(cm^3·s) at Z = 0 to 939 J/(cm^3·s) at Z = 0.15. Greater HRR enables more heat transferred to the nozzle and leads to a higher nozzle temperature; thus, the decreasing influence of fuel-side dilution on TBN is not caused by HRR.

Second, as the flame base always contacts the burner nozzle with or without CO_2 dilutions, as shown in Figure 7, the thermal resistance could be evaluated by DFA. It has been discussed that DFA decreases with the increasing Z for fuel-side dilutions, which enlarges the distance between the flame front and the burner nozzle, and thus the thermal resistance is increased and less heat transfers to the nozzle.

Finally, the fuel flow velocity near the nozzle exit represents the heat dissipation potential of the burner nozzle, and a greater outlet velocity will lead to a lower burner nozzle temperature. Fuel-side dilution increases the velocity of the fuel flow, as presented in Table 3. Therefore, the increasing velocity of the fuel flow for the fuel-side dilutions enhances the heat dissipation potential of the nozzle, leading to a low temperature.

Reponses of HRR, DFA, and U_{fuel} to both air-side and fuel-side CO_2 dilutions and their effects on the burner nozzle temperature are summarized in Table 5. The direction of arrows indicates how they affect: positively (upward), negatively (downward), and negligibly (horizontal). It can be concluded that the suppressed flame attachment and enhanced outlet velocity of the fuel flow account for the greater influence of fuel-side dilution on decreasing the temperature of the burner nozzle. As to the air-side dilutions, the reduced HRR by the increasing of Z is the only reason for the lowered TBN.

Table 5. Different Effects on Burner Nozzle Temperature of CH_4 Flames with and without CO_2 Dilutions

	HRR	DFA	U_{fuel}
fuel-side dilution	enhanced, positive effect ↑	suppressed, negative effect ↓	increased, negative effect ↓
air-side dilution	reduced, negative effect ↓	stable, negligible effect →	stable, negligible effect →

From Figure 9, it can also be observed that H_2O dilution has a similar effect on TBN to CO_2 dilution. TBNs decrease in both sides' dilution with increasing Z and the TBN for fuel-side dilution is lower than that for air-side dilution at the same dilution parameter. For example, when Z = 0.05, the nozzle temperature is 1162 K in fuel-side dilution and 1198 K in air-side dilution; when Z = 0.20, the nozzle temperature is 1037 K in fuel-side dilution and 1136 K in air-side dilution.

The changes in HRR, DFA, and U_{fuel} when H_2O dilutions occur and their effects on the burner nozzle temperature are summarized in Table 6. It was found that the effects of H_2O dilution on TBN are identical to those of CO_2 dilution, and the suppressed flame attachment and enhanced outlet velocity of the fuel flow account for the greater influence of fuel-side dilution on decreasing the temperature of the burner nozzle. Regarding air-side dilutions, the reduced HRR is the only reason for the lowered TBN.

Table 6. Different Effects on Burner Nozzle Temperature of CH_4 Flames with and without H_2O Dilutions

	HRR	DFA	U_{fuel}
fuel-side dilution	enhanced, positive effect ↑	suppressed, negative effect ↓	increased, negative effect ↓
air-side dilution	reduced, negative effect ↓	stable, negligible effect →	stable, negligible effect →

Besides, TBNs of H_2O dilution are lower than those of CO_2 dilution under the same Z conditions from Figure 9, and this result is mainly due to HRR and U_{fuel}. The HRR of H_2O dilution is lower than that of CO_2 dilution, and the velocities of H_2O dilution are more significant than those of CO_2 dilution by comparing Figure 7 with Figure 8. For example, the maximum HRR is 852 J/(cm^3·s) for CO_2 dilution while it reaches a smaller value of 816 J/(cm^3·s) for H_2O dilution in the fuel side.

Based on the above discussion, it is evident that both CO_2 and H_2O dilutions could reduce the nozzle temperature, but the cooling effect in fuel-side dilution is much stronger than that in air-side dilution. Therefore, for the sake of protecting the burner nozzle from high-temperature damage, it is beneficial to add diluents to the fuel stream.

3.5. Flame Height. In the present work, flame height is defined as the HAB of the maximum OH concentration along the central axis. Figure 10 shows the computed flame lengths under different dilution conditions. Flame height increases with the CO_2 addition, and as expected, the flame height for fuel-side dilution is larger than that for air-side dilution with the same dilution parameter. For example, flame heights are

https://doi.org/10.1021/acsomega.3c07406
ACS Omega 2024, 9, 1113−1124

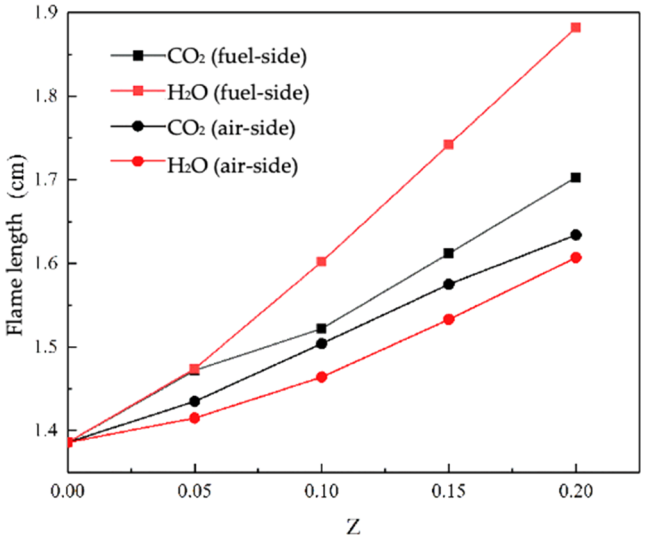

Figure 10. Flame height with CO_2 or H_2O dilutions in fuel side vs air side.

1.472 and 1.435 cm for fuel-side dilution and air-side dilution at $Z = 0.05$, respectively. When $Z = 0.15$, the fuel-side-diluted flame height further increases to 1.612 cm and the air-side-diluted flame height becomes 1.575 cm. Meanwhile, with regard to H_2O dilutions, the flame height increases with increasing Z, and again, the flame heights of fuel-side dilutions are larger than those of air-side dilutions. For example, when $Z = 0.05$, flame heights of fuel-side dilution and air-side dilution are 1.474 cm and 1.415 cm, respectively. When $Z = 0.15$, flame heights of fuel-side dilution and air-side dilution are 1.742 and 1.533 cm, respectively. Obviously, flame heights of CO_2 dilutions are less than those of H_2O dilutions in fuel side but larger than those of H_2O dilutions in air side.

According to the flame height equation developed by Roper,[30] as shown in eq 2, the flame height (L_f) is directly proportional to the volume flow rate of the fuel jet, and because the cross-sectional areas of fuel and air tube were fixed for the jet burner investigated in this research, the volume flow rate of the fuel jet mainly depends on the jet velocity of the fuel stream.

$$L_f \approx \frac{3}{8\pi}\frac{1}{D}\frac{Q_F}{Y_{F,stoic}} \quad (2)$$

where Q_F is the total volume flow rate of fuel stream; D is a mean coefficient diffusion of fuel and oxidant; and $Y_{F,stoic}$ is the stoichiometric mass fraction of the fuel, calculated as the ratio of the fuel stream mass to the oxidizer stream mass in the stoichiometric condition.

Three factors dominate flame height calculations according to eq 2. The jet velocity of the fuel stream is given in Table 3. When dilution occurs in fuel side, the jet velocity of H_2O dilution is larger than that of CO_2 dilution, as discussed in Sections 3.3 and 3.4. For example, the maximum jet velocity increases from 29.63 cm/s at $Z = 0$ to 59.12 cm/s (200% of $Z = 0$) at $Z = 0.15$ for CO_2 dilution cases, while the jet velocity in H_2O dilution is more significantly increased to 101.71 cm/s (342% of $Z = 0$) at the same Z. The stoichiometric mass fractions of the fuel flows only change slightly, for example, 5.5% at $Z = 0$, 5.5% at $Z = 0.05$, and 5.4% at $Z = 0.15$, and similar trends are observed for the stoichiometric mass fraction of CH_4 with H_2O dilutions. Besides, considering the decreasing molecular weight of CO_2, N_2, and H_2O, adding H_2O leads to a higher D while the addition of CO_2 lowers it. Based on above analyses, it can be concluded that the jet velocity is responsible for the flame height in fuel-side dilution.

For air-side dilutions, the fuel jet velocities were fixed for all levels of dilution, i.e., 29.63 cm/s from $Z = 0$ to $Z = 0.15$ for both CO_2 and H_2O dilutions; however, the stoichiometric mass fraction of fuel decreases from 5.5% at $Z = 0$ to 5.2% at $Z = 0.05$ and 4.8% at $Z = 0.15$ when diluted with either CO_2 or H_2O. When taking the effect of diffusion coefficient into account, it is fairly evident that the main factor affecting flame height for air-side dilutions is identified as the stoichiometric mass fraction of fuel, and the greater diffusion coefficient D of H_2O/air than CO_2/air results in a longer flame height of CO_2 dilution than H_2O dilution.

4. CONCLUSIONS

In this study, the influence of dilution strategies on the structure and length of methane coflow diffusion flames at 1 atm and 400 K was numerically studied using an NRC 2D flame program. Two kinds of diluents, CO_2 and H_2O, were investigated. A systematic examination of OH formation, flame attachment, nozzle temperature, and flame height was conducted, with an emphasis on comparing the effects of air-side dilution and fuel-side dilution. Additionally, the distinctions between CO_2 dilution and H_2O dilution were elucidated. Based on these numerical studies, the main findings can be summarized as follows:

(1) Air-side dilution has a greater influence on decreasing OH formation than fuel-side dilution as a result of a larger amount of diluents, and OH formation is reduced through $O + CH_4 = OH + CH_3$ and $H + O_2 = O + OH$. Similarly, because of the much larger amount of injected H_2O than that of CO_2 at the same Z, H_2O dilution generally has a more significant effect on decreasing OH formation than CO_2, except for the fuel-side dilution with a small amount of H_2O addition which is caused by the different chemical effects of the diluents.

(2) The depths of flame attachment decrease with Z for fuel-side dilutions but remain almost unchanged for air-side dilutions. The result shows that the enhanced penetration of the fuel through the convection toward the outside of the burner cannot overwhelm the suppressed the mass diffusion, leading to inhibiting the influence of fuel-side dilutions on flame attachment.

(3) Temperatures of burner nozzle decrease with the dilution ratio, and a greater impact was observed for fuel-side dilutions. Reasons behind this are the suppressed flame attachment and enhanced outlet velocity of the fuel flow account for the greater influence of fuel-side dilution, while TBN is lowered only by the reduced HRR for air-side dilutions.

(4) Adding diluents increases the flame height, and the effect is more profound for fuel-side dilutions than that for air-side dilutions. The jet velocity of the fuel stream dominates the flame height for fuel-side dilutions while the mass fraction of the fuel has significant influence for air-side dilutions. The diffusion coefficient is the primary factor causing the differences between CO_2 and H_2O dilutions, especially for air-side dilutions.

https://doi.org/10.1021/acsomega.3c07406
ACS Omega 2024, 9, 1113−1124

AUTHOR INFORMATION

Corresponding Author

Zhiqiang Wang − *National Engineering Laboratory for Reducing Emissions from Coal Combustion, School of Energy and Power Engineering, Shandong University, Jinan, Shandong 250061, P. R. China*; Email: jackywzq@sdu.edu.cn

Authors

Huanhuan Xu − *National Engineering Laboratory for Reducing Emissions from Coal Combustion, School of Energy and Power Engineering, Shandong University, Jinan, Shandong 250061, P. R. China*; orcid.org/0000-0003-1247-6287

Guangdong Zhou − *School of Energy Science and Engineering, Harbin Institute of Technology, Harbin, Heilongjiang 150001, P. R. China*; orcid.org/0000-0002-3431-3748

Zilin Zhu − *School of Energy Science and Engineering, Harbin Institute of Technology, Harbin, Heilongjiang 150001, P. R. China*

Complete contact information is available at: https://pubs.acs.org/10.1021/acsomega.3c07406

Author Contributions

The manuscript was written through contributions of all authors. All authors have given approval to the final version of the manuscript. The authorship contributions are as follows: H.X.: conceptualization, writing-revision, supervision; G.Z.: investigation, writing-original draft; Z.Z.: visualization, validation; Z.W.: conceptualization, resources.

Notes

The authors declare no competing financial interest.

ACKNOWLEDGMENTS

This work was financially supported by the National Natural Science Foundation of China (Grant No. 52206160), China Postdoctoral Science Foundation (2020M672059), and the Fundamental Research Funds of Shandong University, Shandong Provincial Natural Science Foundation of China (Grant No. ZR2020QE198). Huanhuan Xu also acknowledges the support from Alexander von Humboldt Foundation.

REFERENCES

(1) Hu, M.; Qiao, H.; Du, X. Numerical simulations of the influence of flue gas recycle on nitrogen oxide formation in boiler. *J. North China Electr. Power Univ.* **2007**, *34* (6), 77−82.

(2) Liu, Z.; Song, Q.; Yao, Q.; Zhang, L. Oxy-fuel combustion technology and the production and control of its pollutants. *J. North China Electr. Power Univ.* **2007**, *34* (1), 82−88.

(3) Chen, D.; Ye, T.; Li, H. Review on low NOx combustion techniques *Therm. Power Gener.* 2017.

(4) Cui, M.; Li, X.; Miao, P. Research progress of low NOx gas combustion technology. *Clean Coal Technol.* **2020**, *26* (2), 24−33.

(5) Shao, W.; Liu, S.; Zhang, Z.; Xiao, Y. Influence of the Uniformity of Steam Diluted on the Emissions Characteristics of the Pollutants from a Natural Gas Diffused Flames. *J. Eng. Therm. Energy Power* **2018**, *33* (4), 103−109.

(6) Liu, Q.; Xu, G.; Fang, A.; Nie, C. Experimental Studies on Combustion Characteristic with Steam Dilution to Decrease NOx Emission in Facility Combustor. *J. Eng. Thermophys.* **2007**, *28* (4), 695−698.

(7) Xue, R.; Hu, C. B.; Shi, S.; Pericle, P. Numerical investigation of steam diluent effect on flow field and NOx emissions for diffusion combustors. *J. Propul. Technol.* **2015**, *36* (2), 238−245.

(8) Cho, E.-S.; Chung, S. H. Characteristics of NOx emission with flue gas dilution in air and fuel sides. *KSME Int. J.* **2004**, *18*, 2303−2309.

(9) Feese, J. J.; Turns, S. R. Nitric oxide emissions from laminar diffusion flames: effects of air-side versus fuel-side diluent addition. *Combust. Flame* **1998**, *113* (1−2), 66−78.

(10) Lock, A.; Briones, A. M.; Aggarwal, S. K.; Puri, I. K.; Hegde, U. Liftoff and extinction characteristics of fuel-and air-stream-diluted methane−air flames. *Combust. Flame* **2007**, *149* (4), 340−352.

(11) Marin, M.; Baillot, F. Experimental study of the lifting characteristics of the leading-edge of an attached non-premixed jet-flame: Air-side or fuel-side dilution. *Combust. Flame* **2016**, *171*, 264−280.

(12) Erete, J. I.; Hughes, K. J.; Ma, L.; Fairweather, M.; Pourkashanian, M.; Williams, A. Effect of CO_2 dilution on the structure and emissions from turbulent, non-premixed methane−air jet flames. *J. Energy Inst.* **2017**, *90* (2), 191−200.

(13) Liu, Y.; Xue, Q.; Zuo, H.; et al. Effects of CO_2 and N_2 Dilution on the Combustion Characteristics of H_2/CO Mixture in a Turbulent, Partially Premixed Burner. *ACS Omega* **2021**, *6* (24), 15651−15662.

(14) Vandel, A.; Cano, J. C.; de Persis, S.; Cabot, G. Study of the influence of water vapour and carbon dioxide dilution on flame structure of swirled methane/oxygen-enriched air flames. *Exp. Therm. Fluid Sci.* **2020**, *113*, No. 110010.

(15) Liu, F.; Guo, H.; Smallwood, G. J.; Gülder, Ö. L. The chemical effects of carbon dioxide as an additive in an ethylene diffusion flame: implications for soot and NOx formation. *Combust. Flame* **2001**, *125* (1−2), 778−787.

(16) Wang, L.; Liu, Z.; Chen, S.; Zheng, C.; Li, J. Physical and chemical effects of CO_2 and H_2O additives on counterflow diffusion flame burning methane. *Energy Fuels* **2013**, *27* (12), 7602−7611.

(17) Watanabe, H.; Marumo, T.; Okazaki, K. Effect of CO_2 Reactivity on NOx Formation and Reduction Mechanisms in O_2/CO_2 Combustion. *Energy Fuels* **2012**, *26* (2), 938−951.

(18) Glarborg, P.; Bentzen, L. L. Chemical effects of a high CO_2 concentration in oxy-fuel combustion of methane. *Energy Fuels* **2008**, *22* (1), 291−296.

(19) Min, J.; Baillot, F.; Guo, H.; Domingues, E.; Talbaut, M.; Patte-Rouland, B. Impact of CO_2, N_2 or Ar diluted in air on the length and lifting behavior of a laminar diffusion flame. *Proc. Combust. Inst.* **2011**, *33* (1), 1071−1078.

(20) Tu, Y.; Liu, H.; Yang, W. Flame characteristics of CH_4/H_2 on a jet-in-hot-coflow burner diluted by N_2, CO_2, and H_2O. *Energy Fuels* **2017**, *31* (3), 3270−3280.

(21) Xu, H.; Liu, F.; Sun, S.; Zhao, Y.; Meng, S.; Tang, W. Effects of H_2O and CO_2 diluted oxidizer on the structure and shape of laminar coflow syngas diffusion flames. *Combust. Flame* **2017**, *177*, 67−78.

(22) Cepeda, F.; Jerez, A.; Demarco, R.; Liu, F.; Fuentes, A. Influence of water-vapor in oxidizer stream on the sooting behavior for laminar coflow ethylene diffusion flames. *Combust. Flame* **2019**, *210*, 114−125.

(23) Xu, H.; Liu, F.; Wang, Z.; Ren, X.; Chen, J.; Li, Q.; Zhu, Z. A detailed numerical study of NOx kinetics in counterflow Methane diffusion flames: effects of fuel-side versus oxidizer-side dilution. *J. Combust.* **2021**, *2021*, No. 6642734, DOI: 10.1155/2021/6642734.

(24) Liu, F.; Thomson, K. A.; Guo, H.; Smallwood, G. J. Numerical and experimental study of an axisymmetric coflow laminar methane−air diffusion flame at pressures between 5 and 40 atm. *Combust. Flame* **2006**, *146* (3), 456−471.

(25) Liu, F.; Consalvi, J.-L.; Fuentes, A. Effects of water vapor addition to the air stream on soot formation and flame properties in a laminar coflow ethylene/air diffusion flame. *Combust. Flame* **2014**, *161* (7), 1724−1734.

(26) Liu, F.; Guo, H.; Smallwood, G. J. Effects of radiation model on the modeling of a laminar coflow methane/air diffusion flame. *Combust. Flame* **2004**, *138* (1−2), 136−154.

(27) Guo, H.; Liu, F.; Smallwood, G. J.; Gülder, Ö. L. A numerical investigation of thermal diffusion influence on soot formation in

ethylene/air diffusion flames. *Int. J. Comput. Fluid Dyn.* **2004**, *18* (2), 139−151.
(28) Xu, H.; Liu, F.; Sun, S.; Zhao, Y.; Meng, S.; Tang, W.; Feng, D.; Gu, M. Influence of preheating and burner geometry on modeling the attachment of laminar coflow CH_4/air diffusion flames. *Combust. Flame* **2018**, *191*, 381−393.
(29) Li, Z.; Lou, C.; Kumfer, B. M. Revealing the competitive relationship between soot formation and chemiluminescence. *Combust. Flame* **2022**, *245*, No. 112335.
(30) Roper, F. The prediction of laminar jet diffusion flame sizes: Part I. Theoretical model. *Combust. Flame* **1977**, *29*, 219−226.

https://doi.org/10.1021/acsomega.3c07406
ACS Omega 2024, 9, 1113−1124